Ocean Engineering 264 (2022) 112527

Contents lists available at ScienceDirect

Ocean Engineering

journal homepage: www.elsevier.com/locate/oceaneng

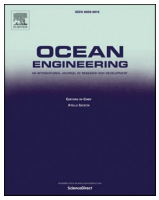

A modified breaker index formula for depth-induced wave breaking in spectral wave models

Zereng Chen [a], Qinghe Zhang [a,*], Yongsheng Wu [b], Chao Ji [c]

[a] State Key Laboratory of Hydraulic Engineering Simulation and Safety, Tianjin University, Tianjin, 300072, China
[b] Fisheries and Oceans Canada, Bedford Institute of Oceanography, Dartmouth, Nova Scotia, B2Y 4A2, Canada
[c] National Engineering Research Center of Port Hydraulic Construction Technology, Tianjin Research Institute for Water Transport Engineering, Ministry of Transport, Tianjin, 300456, China

ARTICLE INFO

Keywords:
SWAN
Coastal water
Breaker index
Mild beach slopes

ABSTRACT

The breaker index, defined as the ratio of wave height to local water depth for incipient breaking, is a key parameter in contemporary spectral wave models. In the present study, we modified the breaker index of Goda's formula using the SWAN model (Simulating WAves Nearshore). We suggested that the breaker index is a function of the deep-water wave steepness, bottom slope and relative water depth. The formula is evaluated against observational data, and the evaluation indicates that the modeled wave heights using the formula are significantly improved, especially for cases over mild and flat slopes. The formula is further evaluated through comparisons with published formulas and the improved formula overall shows better performance.

1. Introduction

Breaking waves due to shallowing water depths are common in nearshore waters (Holthuijsen, 2007). Depth-induced wave breaking is a vital process in coastal engineering because wave breaking generates energy dissipation and currents, which are important for environmental issues and human activities in coastal waters, for example, infrastructure design, navigation safety, pollutant dispersion and sediment transport (Svendsen, 1984; Lin and Liu, 1998; Salmon and Holthuijsen, 2015; Lin et al., 2020, 2021; Varing et al., 2020). In spectral wave models such as SWAN (Simulating WAves Nearshore), the criterion to determine wave breaking is usually parameterized as the ratio of the maximum wave height to the local water depth. The ratio is a dimensionless parameter and is commonly called the breaker index (Camenen and Larson, 2007; Zhang et al., 2021). The criterion of the maximal wave height before breaking is a function of the breaker index provided that local morphological change is negligible. In the literature, methods to determine the value of the breaker index, differ from a constant approximation to functions of parameters of waves, beach slopes and water depth, depending on specific purposes (Battjes and Stive, 1985; Nelson, 1987; Ruessink et al., 2003). The breaker index is important in a spectral wave model, and its value should be treated carefully due to the complexity of the wave conditions (Baldock et al., 1998; Apotsos et al., 2008).

Using field observations, laboratory experiments and numerical models, a number of parameterization formulas of the breaker index have been implemented. For example, Battjes and Janssen (1978, hereafter BJ78) suggested a constant value of 0.8 for the breaker index based on *in-situ* observed and laboratory experimental wave heights. Based on a more comprehensive dataset, Battjes and Stive (1985) proposed a parameterization formula to include the effect of the incident wave steepness, in which the breaker index varies with the deep-water wave steepness. Nelson (1987) also indicated that the breaker index is a variable and is a function of the beach slope. Based on field observations, Ruessink et al. (2003) considered the breaker index as a function of the normalized water depth, which equals the product of local water depth and wavenumber. In contrast, Salmon et al. (2015, hereafter SA15) proposed the breaker index as a function of the beach slope and the local water depth. Lin and Sheng (2017, hereafter LS17) suggested a nonlinear term of the beach slope based on SA15. Using field observations and large numbers of laboratory data, Goda (1975) developed a parameterization formula of the breaker index as a function of water depth, deep-water wave length, beach slope and an empirical coefficient. Based on the reanalysis of the field data used in Goda (1975), the formula was updated by decreasing the contribution of the beach slope

* Corresponding author.
E-mail address: qhzhang@tju.edu.cn (Q. Zhang).

https://doi.org/10.1016/j.oceaneng.2022.112527
Received 7 April 2022; Received in revised form 11 August 2022; Accepted 7 September 2022
Available online 16 September 2022

Notations

A =	proportionality coefficient of breaker index formula
d =	water depth where waves break
h =	local water depth
H_{max} =	the maximal wave height defined by Eq. (6)
H_{rms} =	the root-mean-square wave height
H_s =	the significant wave height
H_{s0} =	the significant wave height in deep water
k =	local wave number
L_0 =	the deepwater wavelength defined by Eq. (8)
m =	beach slope
s_0 =	the deepwater wave steepness
T_p =	the peak period based on the incident wave conditions

Table 1
The empirical coefficient A for random waves.

	Range of A	Value for use
Goda (1975)	0.12–0.18	Adjusted empirically
Kriebel (2000)	0.09–0.18	0.142
Li et al. (2000)	–	0.15 (0.12)
Wu et al. (1985)	–	Calculated
Goda (2010)	0.12–0.18	Adjusted empirically
Shen et al. (2017)	–	Calculated
Lin and Sheng (2017)	–	0.17

(Goda, 2010, hereafter G10). Using model comparisons, SA15, LS17 and Tomasicchio et al. (2020) noted that breaker index formulas show better performance when the effects of both the beach slope and relative water depth are considered. Detailed comparisons of the formulas above can be found in SA15 and LS17.

In the present study, we focus on the work of Goda. The formula of Goda (1975) has been extensively applied to coastal studies (Liu et al., 2011), for example, estimating wave heights (Goda, 2009; Kang et al., 2020), simulating waves breaking on sloping beaches (Izumiya and Isobe, 1986), determining the breaking point (Sakai et al., 1988), predicting overtopping and wave forces (Allsop et al., 1998), and investigating wave breaking over sandy beaches (Udo and Mano, 2010). The better performance of G10 has been proven by coastal scientists (Yao et al., 2013; Salvadori et al., 2014; Robertson et al., 2015). G10 is a comprehensive formula that relates the wave height at breaking to the local water depth and the beach slope. The formula can be applied to the slopes not only in sandy beach slope cases but also in mild slopes as low as 1:200. Using the SWAN model, Shen et al. (2017) calibrated the empirical parameter of Goda (1975) with bottom slopes from 1:20 to 1:38. They found that the parameter is a function of the deep-water wave steepness. LS17 suggested that G10 is one of the best parameterizations in sloping and barred bottom cases. At the same time, Lin and Sheng (2017) also noted that G10 has significant errors when it is applied to cases with flat bottoms. As we know, the empirical coefficient in G10 controls the contributions of the wave parameters, the beach slope and water depth. The coefficient is a key in the formula; however, its value varies over a relatively large range, and how to determine its value is still under discussion. Therefore, using models and laboratory experimental data, we revisit the empirical coefficient in G10 and attempt to improve the G10 model in the application of spectral wave models, especially for mild slopes and flat bottoms.

The structure of this paper is as follows. Section 2 describes the numerical models and data, and the results and discussions are shown in Sections 3 and 4, respectively. The conclusions are presented in Section 5.

2. Models and data

2.1. Models

SWAN (version 41.31) is a third-generation wave model that simu-

Table 2
Summary of random wave conditions and deep-water wave steepness. The fourth column is the water depth at the location of the wavemaker. H_s is the significant wave height. (The range of deep-water wave steepness is 0.0092–0.0458, and the incident peak period is 1.1–2.4 s)

Case	Incident H_s (m)	T_p (s)	Depth (m)	Deep-water wave steepness	Bottom profile
a	0.120	1.7	0.35	0.0278	1/100
b	0.120	2.1	0.35	0.0171	1/100
c	0.120	2.4	0.35	0.0125	1/100
d	0.150	1.5	0.35	0.0458	1/100
e	0.100	1.3	0.30	0.0411	1/120
f	0.100	1.5	0.30	0.0301	1/120
g	0.120	1.6	0.30	0.0312	1/120
h	0.125	2.4	0.30	0.0126	1/120
i	0.110	1.6	0.25	0.0279	1/150
j	0.120	2.3	0.25	0.0129	1/150
k	0.105	2.4	0.25	0.0102	1/150
l	0.080	1.7	0.20	0.0170	1/200
m	0.080	2.0	0.20	0.0115	1/200
n	0.080	2.2	0.20	0.0092	1/200
o	0.050	1.5	0.20	0.0142	1/200
p	0.040	1.1	0.12	0.0215	1/300
q	0.040	1.3	0.12	0.0146	1/300
r	0.040	1.5	0.12	0.0104	1/300

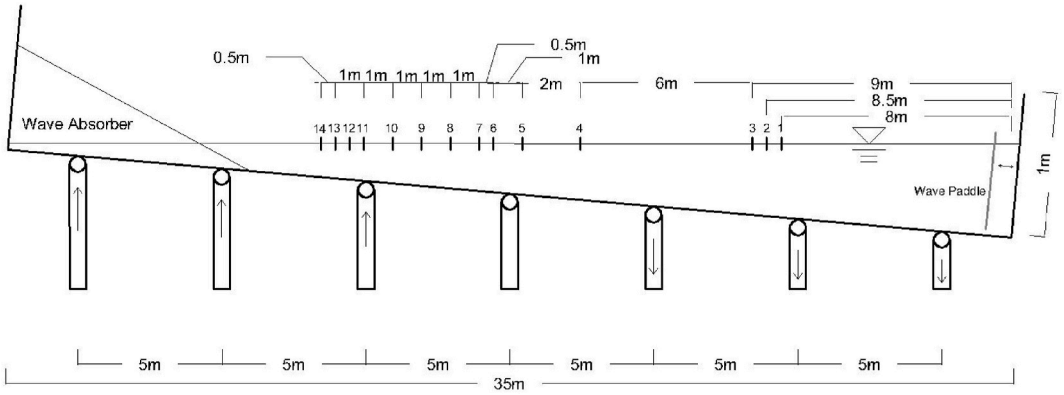

Fig. 1. Schematic diagram of the wave tank with a total of 14 wave gauges. The wave paddle at the right end is denoted as 0 m.

Table 3
Observational data of the 18 cases.

Case	Slope	Wave gauge and the observational H_s (m)													
		1	2	3	4	5	6	7	8	9	10	11	12	13	14
a	1:100	0.113	0.109	0.111	0.099	0.091	0.089	0.086	0.081	0.081	0.075	0.067	0.064	0.060	0.061
b	1:100	0.116	0.114	0.112	0.102	0.095	0.090	0.090	0.080	0.076	0.071	0.066	0.065	0.062	0.063
c	1:100	0.118	0.117	0.119	0.103	0.093	0.094	0.090	0.083	0.078	0.074	0.071	0.071	0.069	0.064
d	1:100	0.122	0.122	0.120	0.101	0.094	0.089	0.086	0.083	0.077	0.072	0.067	0.066	0.061	0.061
e	1:120	0.089	0.090	0.090	0.081	0.075	0.075	0.073	0.067	0.063	0.057	0.054	0.053	0.049	0.050
f	1:120	0.094	0.095	0.090	0.085	0.081	0.080	0.078	0.072	0.069	0.065	0.054	0.054	0.053	0.054
g	1:120	0.098	0.100	0.094	0.079	0.076	0.079	0.075	0.066	0.062	0.062	0.057	0.055	0.059	0.056
h	1:120	0.109	0.110	0.109	0.091	0.082	0.080	0.076	0.072	0.072	0.070	0.070	0.063	0.058	0.060
i	1:150	0.085	0.086	0.086	0.074	0.069	0.068	0.066	0.062	0.063	0.057	0.055	0.052	0.049	0.047
j	1:150	0.092	0.093	0.091	0.076	0.070	0.067	0.069	0.063	0.059	0.057	0.053	0.052	0.049	0.049
k	1:150	0.094	0.092	0.089	0.076	0.071	0.068	0.069	0.063	0.059	0.059	0.056	0.055	0.052	0.053
l	1:200	0.070	0.068	0.068	0.056	0.052	0.054	0.052	0.046	0.045	0.045	0.042	0.039	0.039	0.038
m	1:200	0.069	0.069	0.071	0.058	0.057	0.051	0.051	0.051	0.049	0.046	0.041	0.041	0.039	0.039
n	1:200	0.070	0.067	0.067	0.060	0.053	0.053	0.053	0.050	0.050	0.048	0.041	0.043	0.040	0.040
o	1:200	0.051	0.053	0.052	0.051	0.047	0.046	0.046	0.044	0.045	0.040	0.040	0.040	0.040	0.040
p	1:300	0.035	0.034	0.035	0.030	0.028	0.027	0.027	0.025	0.024	0.021	0.020	0.020	0.019	0.018
q	1:300	0.036	0.035	0.035	0.031	0.029	0.026	0.025	0.024	0.024	0.020	0.019	0.020	0.019	0.019
r	1:300	0.036	0.035	0.035	0.030	0.028	0.028	0.028	0.026	0.024	0.021	0.020	0.020	0.019	0.017

Table 4
Summary of laboratory and field observational data from 21 cases. Column 5 shows the deep-water wave steepness ranging from 0.0011 to 0.0419. Column 7 includes different kinds of bottom profiles, with bottom slopes ranging from 1:10 to 1:80.

Case	Name	Data source	Incident wave H_s (m)	Deep-water wave steepness	Optimal A	Bottom profile	Beach type
a	Eldeberky	Eldeberky (2011)	0.580	0.0055	0.136	Barred beach	Field
b	MK92a	Mase and Kirby (1992)	0.040	0.0099	0.147	Slope, 1:20	Small-scale
c	MK92b	Mase and Kirby (1992)	0.040	0.0270	0.159	Slope, 1:20	Small-scale
d	J2	Baldock et al. (1998)	0.105	0.0319	0.163	Slope, 1:20 to 1:10	Small-scale
e	J1	Baldock et al. (1998)	0.127	0.0388	0.166	Slope, 1:20 to 1:10	Small-scale
f	J3	Baldock et al. (1998)	0.065	0.0419	0.168	Slope, 1:20 to 1:10	Small-scale
g	J6033A	Baldock and Huntley (2002)	0.141	0.0355	0.165	Slope, 1:10	Small-scale
h	J6033B	Baldock and Huntley (2002)	0.106	0.0266	0.161	Slope, 1:10	Small-scale
i	J6033C	Baldock and Huntley (2002)	0.071	0.0178	0.153	Slope, 1:10	Small-scale
j	Ting01	Ting (2001)	0.152	0.0253	0.160	Slope, 1:35	Small-scale
k	Fernando1	Mendez and Losada (2004)	0.150	0.0074	0.141	Sandy beach	Large-scale
l	Fernando2	Mendez and Losada (2004)	0.220	0.0236	0.155	Sandy beach	Large-scale
m	Fernando3	Mendez and Losada (2004)	0.125	0.0062	0.135	Sandy beach	Large-scale
n	R13A1	Ruessink et al. (2013)	0.100	0.0282	0.160	Slope, 1:80	Large-scale
o	R13A2	Ruessink et al. (2013)	0.200	0.0273	0.159	Slope, 1:80	Large-scale
p	test3	Alsina and Baldock (2007)	0.849	0.0080	0.146	Sandy beach	Field
q	Guza-2	Wu et al. (1985)	0.523	0.0011	0.110	Sandy beach	Field
r	Guza-3	Wu et al. (1985)	0.707	0.002	0.122	Sandy beach	Field
s	Guza-4	Wu et al. (1985)	0.735	0.0021	0.125	Sandy beach	Field
t	Guza-5	Wu et al. (1985)	0.566	0.0021	0.125	Sandy beach	Field
u	Guza-6	Wu et al. (1985)	0.368	0.0017	0.120	Sandy beach	Field

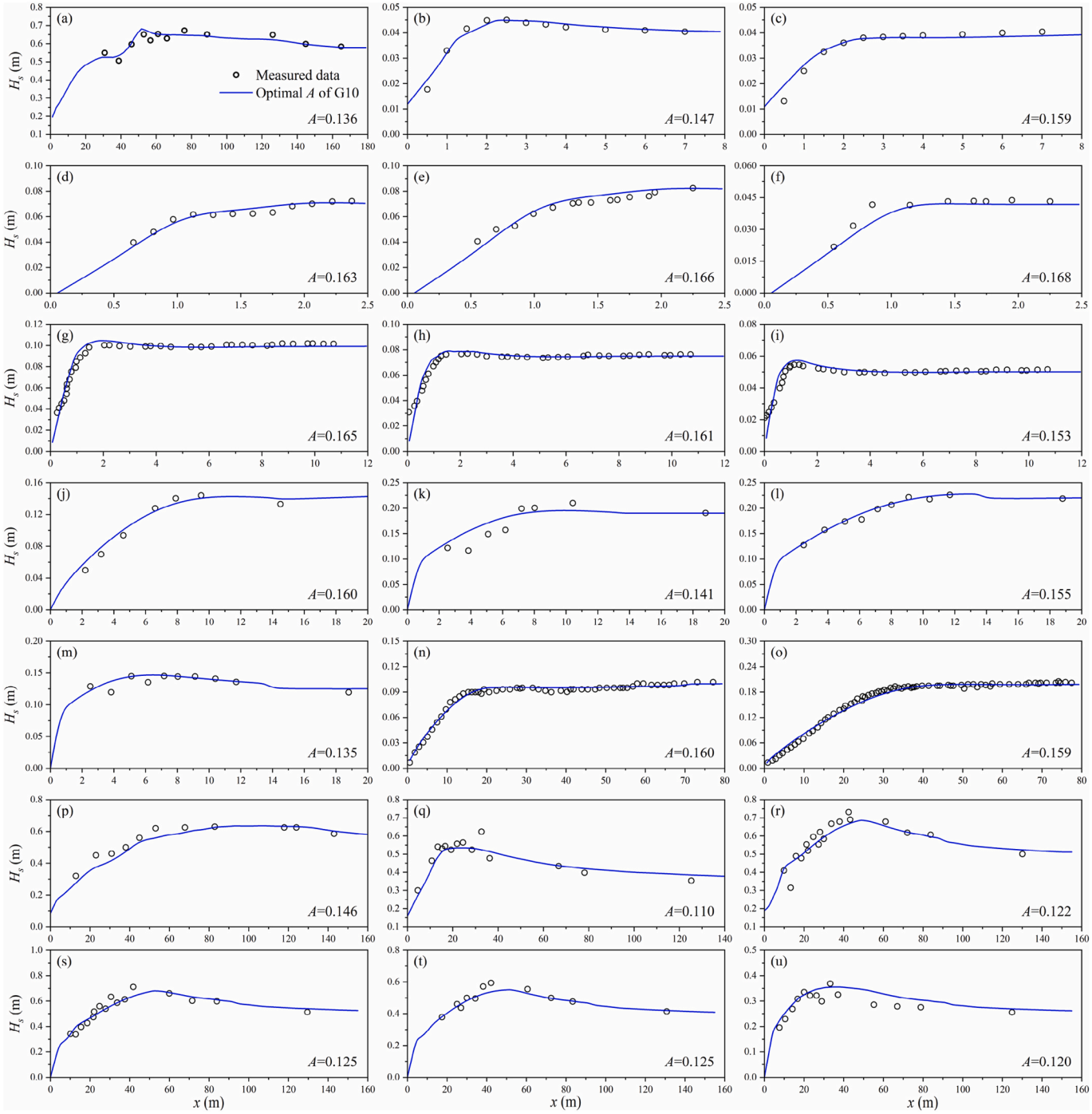

Fig. 2. Simulation results of 21 cases. Lines are the model results choosing the optimal A of G10, while the circles are measured data. The number from a to u in the figure corresponds with Table 4.

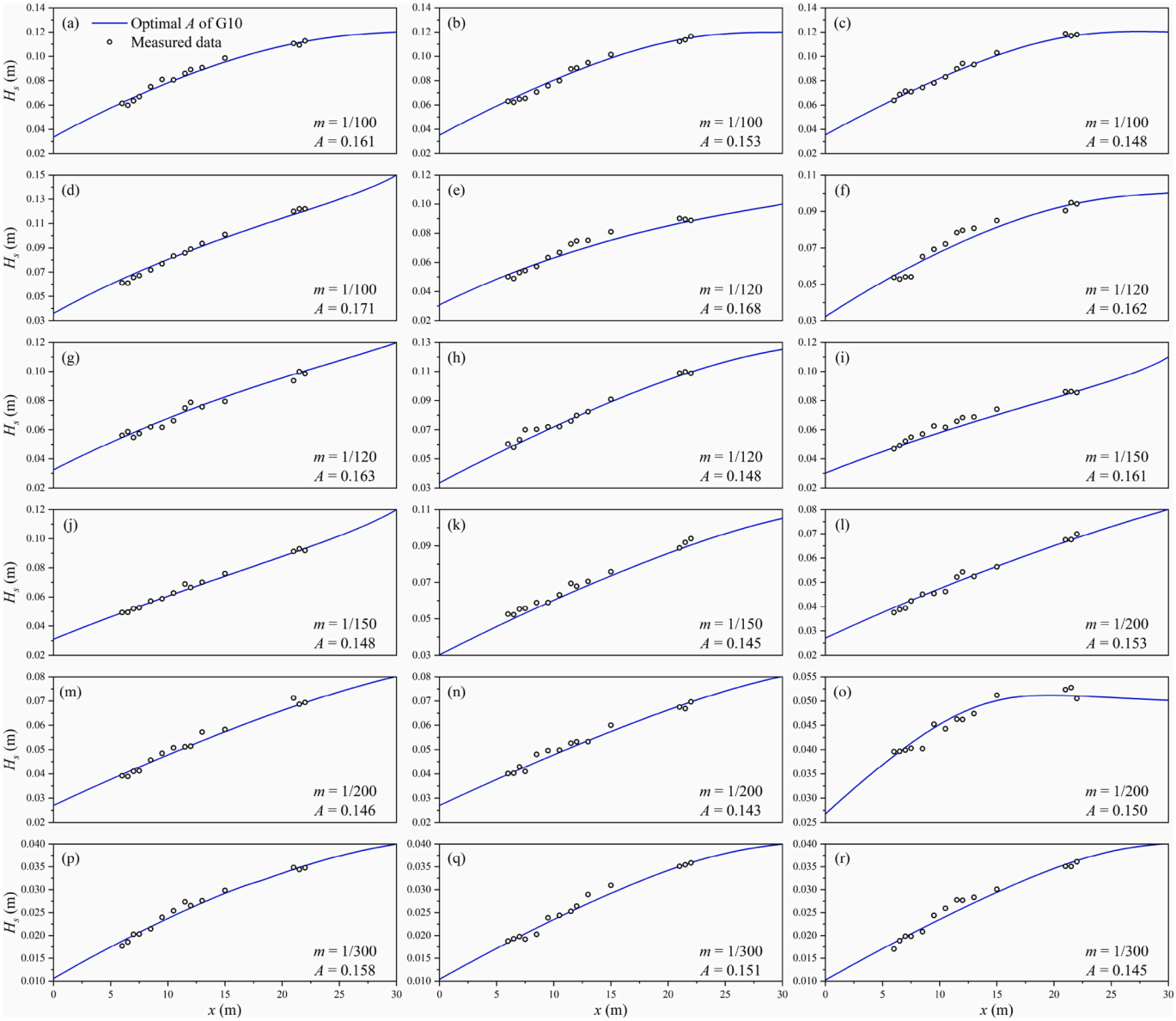

Fig. 3. Simulation results of 18 cases in Table 3. Lines are the model results choosing the optimal A of G10, while the circles are measured data. The numbers from a to r in the figure correspond with Table 3.

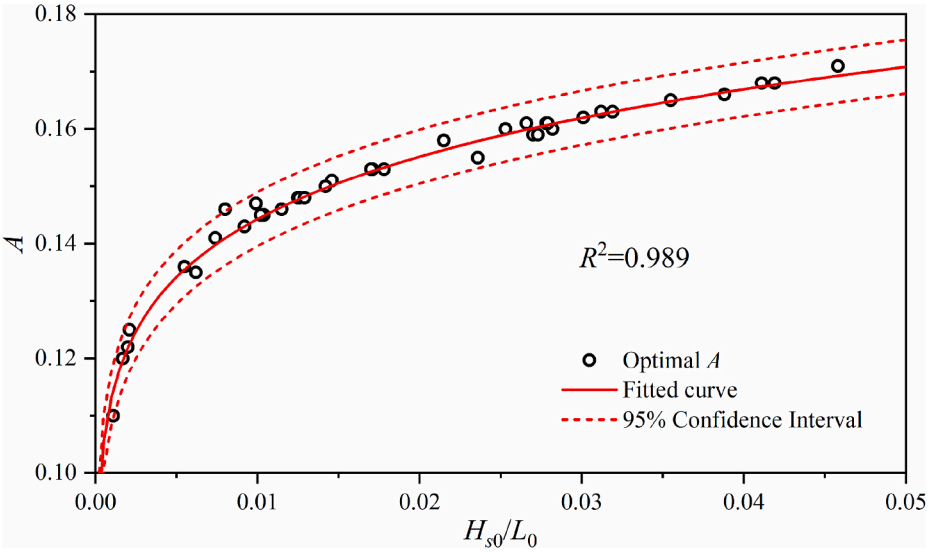

Fig. 4. The relationship between the deep-water wave steepness and the optimal A in G10. The red line is the fitted curve with $R^2 = 0.989$, and the black dots are the optimal results of all the cases. The red dashed lines are the 95% confidence intervals. (For interpretation of the references to colour in this figure legend, the reader is referred to the Web version of this article.)

lates the propagation of wave spectra in near-shore waters (Booij et al., 1999). In the model, the wave energy balance equation is written as:

$$\frac{\partial N}{\partial t} + \nabla_{\mathbf{x}} \cdot \left[N\left(\mathbf{c_g} + \mathbf{u}\right)\right] + \frac{\partial N c_\sigma}{\partial \sigma} + \frac{\partial N c_\theta}{\partial \theta} = \frac{S_{\text{tot}}}{\sigma} \tag{1}$$

where N is the wave action density; $\mathbf{c_g}$ is the wave group velocity vector; $\mathbf{u}$ is the current velocity vector; $\mathbf{x}$ contains the x and y directions; and c_σ and c_θ are the velocity components along σ and θ, respectively. The first term on the left of the equation is the change in the density spectrum with respect to time; the second to fourth terms on the left are the change in the density spectrum with respect to the physical and spectral space; the right term is the source term, which contains the following physical mechanisms:

$$S_{\text{tot}} = S_{\text{in}} + S_{\text{nl4}} + S_{\text{wc}} + S_{\text{nl3}} + S_{\text{bot}} + S_{\text{br}} \tag{2}$$

where S_{in} represents the wave generation by wind; S_{nl4} is the quadruplet wave–wave interaction; S_{wc} is the dissipation by white-capping in deep water; S_{nl3} is the triple wave–wave interaction mainly in shallow water; S_{bot} is the dissipation due to the bottom friction; and S_{br} is the dissipation due to depth-induced wave breaking, which is written as:

$$S_{\text{br}} = D_{\text{tot}} \frac{E(\sigma,\theta)}{E_{\text{tot}}} \tag{3}$$

where $E(\sigma,\theta) = \sigma N$, $E_{\text{tot}} = \frac{1}{8} H_{rms}^2$ is the total wave energy (H_{rms} is the root-mean-square wave height), and D_{tot} is the mean dissipation rate of wave energy due to wave breaking. In the literature, there are a number of formations to express D_{tot} (Lin and Sheng, 2017; Rattanapitikon and Duong, 2019). In the present study, we use the commonly used formation of D_{tot} in BJ78, which is rewritten as:

$$D_{\text{tot}} = -\frac{1}{4} \alpha Q_b \frac{\overline{\sigma}}{2\pi} H_{\max}^2 \tag{4}$$

$$\frac{1 - Q_b}{\ln Q_b} = -\left(\frac{H_{rms}}{H_{\max}}\right)^2 \tag{5}$$

$$H_{\max} = \gamma h \tag{6}$$

where α is a constant coefficient, generally taken as 1.0; $\overline{\sigma}$ is the average frequency of the wave energy spectrum; h is the local water depth; and γ is the breaker index. The wave energy dissipation rate can be calculated using Eqs. (3)–(6) as long as γ is known. Hence, we can find that the value of the breaker index is an important parameter in solving the wave equation.

Following Goda (1975, 2010), the formula is reproduced as:

$$\gamma = A\left\{1 - \exp\left[-1.5\pi \frac{d}{L_0}\left(1 + Cm^{4/3}\right)\right]\right\} \Big/ \frac{d}{L_0} \tag{7}$$

$$L_0 = g T_p^2 \Big/ (2\pi) \tag{8}$$

in which d is the water depth where waves break; m is the beach slope; C is an empirical parameter, 15 was used in Goda (1975), and 11 was used in G10; L_0 is the wavelength in deep water, which is calculated by Eq. (8) in the present study, T_p is the peak period based on the incident wave conditions and A is an empirical coefficient.

As we can see, the breaker index of G10 is not only associated with the wave and bathymetry parameters but also related to the empirical parameter A (See Table 1). In the literature, the values of A vary in a range of 0.12–0.18 (Goda, 1975, 2010). Using laboratory experimental data, Kriebel (2000) noted that the value of A varied from 0.090 to 0.180 with a mean of 0.142 with a standard deviation of 0.017 by fitting the experimental data with Eq. (7). Li et al. (2000) also reported that the coefficient value of A is 0.150 with a standard deviation of 0.031. Using the SWAN model, Shen et al. (2017) found that the value of A is a function of deep-water wave steepness. Lin and Sheng (2017) suggested 0.17 in their model comparisons. Deborah J Wood and Oumeraci, 2001 suggested that the value of A varies with the critical wave steepness, defined as the ratio of the breaking wave heights to the deep-water wavelength. In practice, the value of A is calibrated by comparing the modeled wave heights and the observed counterparts. The model is then

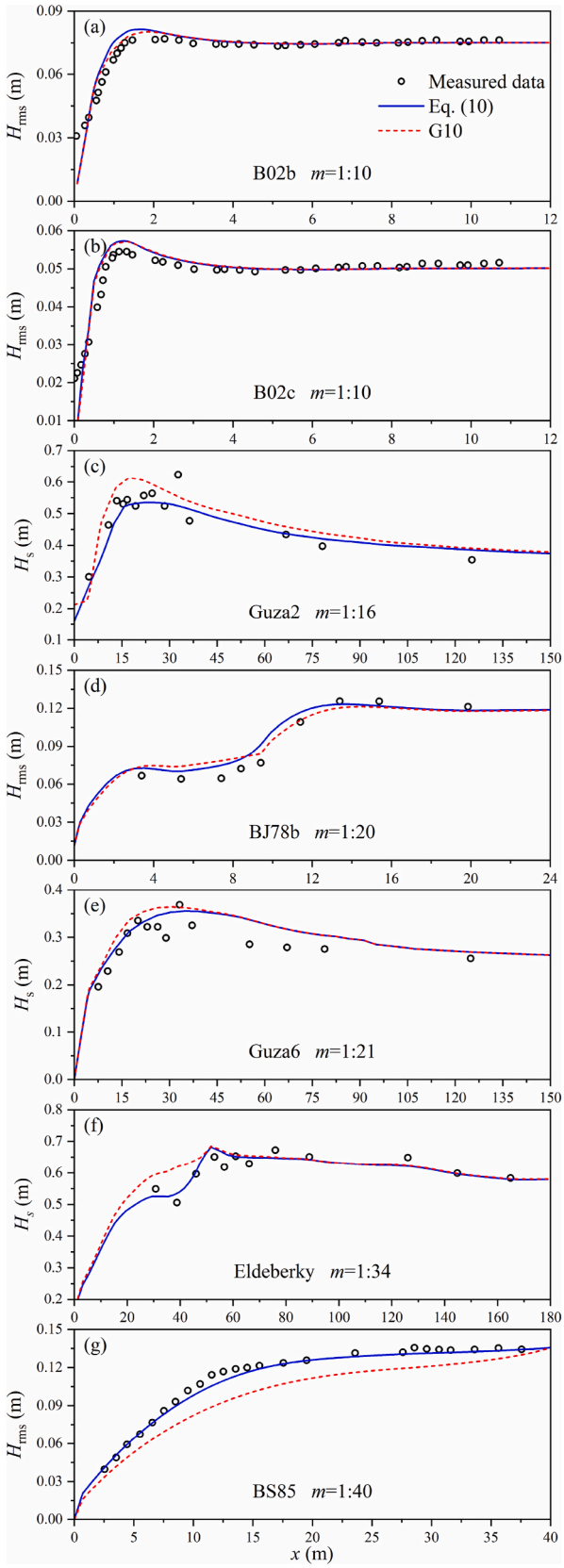

Fig. 5. The simulated wave heights of G10 (red dashed lines) and Eq. (10) (blue lines) under relatively steep slope cases. Black circles: measured data. $x = 0$ m represents the still water depth. (d) and (f) are barred cases, where they have negative slopes. (For interpretation of the references to colour in this figure legend, the reader is referred to the Web version of this article.)

run based on the calibrated value. However, for cases where the observations are not available, the calibration of A is impossible. At the same time, the calibration may become more difficult because of the complicated bathymetry in nearshore waters.

2.2. Experimental wave height data

In addition to the commonly used wave height data at slopes of 1:10–1:100 (e.g. Battjes and Stive (1985), Baldock et al. (1998) and Ruessink et al. (2013)), in the present study, we also carry out experiments in the laboratory at slopes of 1:100–1:300. The wave flume used has a size of 35 m in length, 1 m in width, and 1 m in depth at the State Key Laboratory of Hydraulic Engineering Simulation and Safety at Tianjin University, and its slope is adjustable. A schematic diagram of the experimental setup is shown in Fig. 1. The right end of the flume adopts wave generation, and the left end is the wave absorber. Fourteen wave gauges are set in the wave flume to measure the wave heights. The distance of each support is 5 m. In this paper, the experiments are carried out under uniform slope conditions of 1:100, 1:120, 1:150, 1:200 and 1:300. The wave conditions of the experiments are listed in Table 2, and the measured data are given in Table 3.

3. Results

In this section, we first show the calibration of the breaker index and then investigate the sensitivity of the formula to the formula parameters. In the last subsection, we compare the formula to G10.

3.1. Calibration of the breaker index

Based on the observational data, we tuned the value of A until the 'best' modeled wave heights were obtained. The value of A is defined as the optimal A. The optimal values for all 21 cases are listed in Table 4, and the model-data comparisons with the optimal A are plotted in Fig. 2. In all 21 cases, the still water depth at the location of $x = 0$ m is zero. In case a, there is a sandy bar from $x = 50$–70 m. In cases k–m, the beach slope at $x = 1$ m is steeper. In cases q–u, the incident wave directions are oblique to the shoreline. In addition, using the laboratory data in Table 3, the simulation results of the optimal A are also shown in Fig. 3. The still water depths at $x = 0$ m are 0.05 m, 0.05 m, 0.05 m, 0.05 m and 0.02 m when the beach slope is 1:100, 1:120, 1:150, 1:200 and 1:300, respectively. The modeled wave heights are comparable to the observed wave heights in all cases of various incident wave conditions and bathymetry, where the average error between the modeled and measured wave heights are lower than 5%. We then investigated the relationships between the optimal A and the wave conditions, and we found that A is strongly related to the deep-water wave steepness (Fig. 4). The fitted line is as follows:

$$A = 0.234 s_0^{0.105} \tag{9}$$

where the deep-water wave steepness $s_0 = H_{s0}/L_0$ and H_{s0} is the significant wave height in deep water. Based on the cases in the present study, the value of s_0 is between 0 and 0.05.

In addition to the calibration of the empirical parameter, A, we also adjust the application condition of G10 since the formula is invalid once the slope parameter m is less than zero. To solve this issue, following Nelson (1987), Choi and Yoon (2011) and Choi et al. (2012), we use 0.5 as the breaker index when the beach slope is smaller than 0.002 (including negative slope), so the final formula is given as:

$$\begin{cases} \gamma = 0.234 s_0^{0.105} \left\{ 1 - \exp\left[-1.5\pi \dfrac{d}{L_0} \left(1 + 11 m^{4/3} \right) \right] \right\} \Big/ \dfrac{d}{L_0}, & \text{if } 0.002 < m < 0.1 \\ \gamma = 0.50, & \text{if } m \le 0.002 \end{cases} \tag{10}$$

It can be seen from Eq. (10) that the breaker index can be uniquely

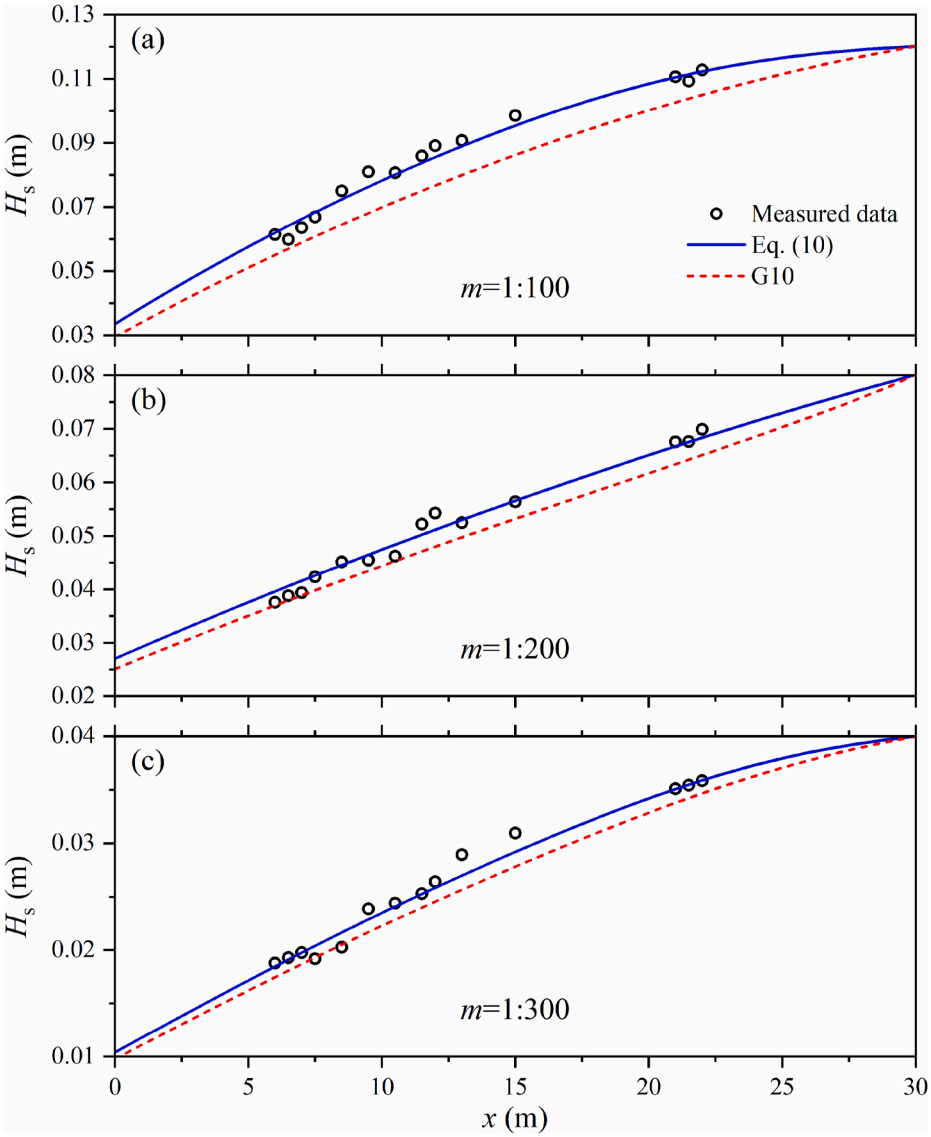

Fig. 6. The simulated wave heights of G10 (red dashed lines) and Eq. (10) (blue lines) under very mild slope cases. Black circles: measured data. (For interpretation of the references to colour in this figure legend, the reader is referred to the Web version of this article.)

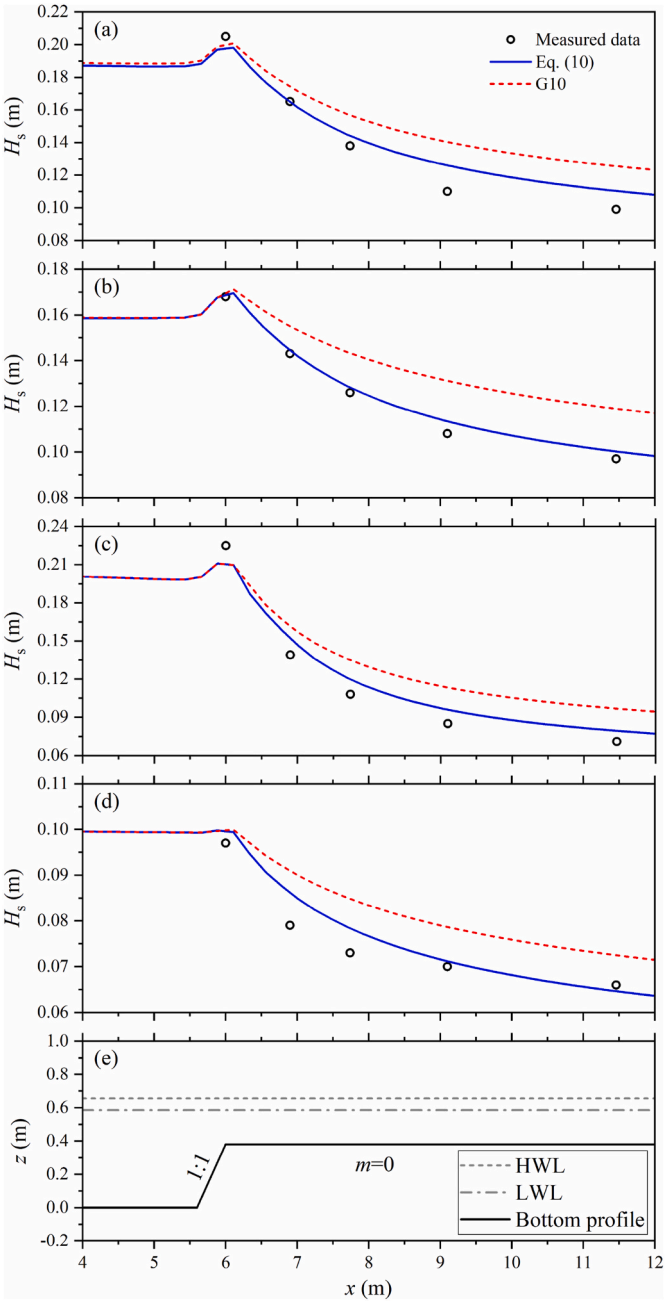

Fig. 7. The simulated wave heights of the four cases in Jensen (2004) by the G10 model and Eq. (10): (a)–(d) are the cases of 1, 4, 18 and 29, respectively. (e) The test bottom profile (black line). The higher water level (HWL, gray dashed line) is 0.655 m, and the lower water level (LWL, gray dash-dotted line) is 0.585 m.

determined based on the deep-water wave steepness (s_0), the beach slopes (m) and the relative water depth (d/L_0). By fixing m and d/L_0, with s_0 varying from 0 to 0.05, the value of the breaker index has a large variation of about 50%, which indicates that using a constant value for parameter A may lead to significant uncertainties in the calculation of the breaker index.

3.2. Comparisons to the G10 model

In this subsection, the performance of Eq. (10) is evaluated by comparing the modeled wave heights to those from the formula of G10, in which A is a constant, 0.142, based on Kriebel (2000). To quantitatively evaluate the comparison, two parameters, the scatter index (SI) and relative bias (RB), are defined and written as:

$$SI = \sqrt{\frac{1}{M}\sum_{i=1}^{M}\left(H_{\mathrm{com},i} - H_{\mathrm{obs},i}\right)^2} \Big/ \overline{H}_{\mathrm{obs}} \tag{11}$$

$$RB = \frac{1}{M}\sum_{i=1}^{M}\left(H_{\mathrm{com},i} - H_{\mathrm{obs},i}\right) \Big/ \overline{H}_{\mathrm{obs}} \tag{12}$$

where M is the number of measured data in each case, H_{com} represents the computed results, H_{obs} represents the observed wave height, and $\overline{H}_{\mathrm{obs}}$ represents the averaged observed wave height.

In the present study, we categorize the comparison into groups in terms of the slopes, Group I (m = 1:10–1:40), Group II (m = 1:100–1:300), and Group III (m = 0). The comparisons of the specific groups are plotted in Figs. 5–7, and the two statistical parameters from Eqs. (11) and (12) are summarized in Table 5. In Group I, both the wave heights from the formula of G10 and Eq. (10) overall agree well with the observations (Fig. 5(a-g)). The comparisons indicate that the performance of Eq. (10) is better for cases with lower slopes (Table 5). In Group II, both formulas agree with the observations as well. However, we can determine that the wave heights from G10 are clearly lower than the observations (Fig. 6). At the same time, the nonlinear variation in the wave heights with the distance, shown in the observations (Fig. 6(a)), is not reproduced using G10. Contrary to Group II, the modeled wave heights with G10 in Group III are clearly higher than those with Eq. (10), although both follow the trend of the observations (Fig. 7). In summary, both the formula of G10 and Eq. (10) well for cases with steep slopes. However, significant improvement can be found from the new formula for cases with relatively mild slopes, especially for the cases with flat bottoms.

4. Discussion

In this section, we discuss the performance of the formula by comparing four published formulas of the breaker index, consisting of the commonly used formula BJ78 (constant value of 0.73) and three recently developed formulas SA15, LS17 and SY17, which are shown in Eqs. 13–16. Detailed description of these specific formula can be found in the literature.

$$\gamma_{BJ} = 0.73 \tag{13}$$

$$\begin{cases} \gamma_{\mathrm{SA15}} = \gamma_1/\tanh(\gamma_1/\gamma_2) \\ \gamma_1 = 0.54 + 7.59m \\ \gamma_2 = -8.06 + 8.09kh \end{cases} \tag{14}$$

$$\begin{cases} \gamma_{\mathrm{LS17}} = \gamma_1/\tanh(\gamma_1/\gamma_2) \\ \gamma_1 = 0.54 + 0.47\exp(-0.018/m) \\ \gamma_2 = -8.06 + 8.09kh \end{cases} \tag{15}$$

$$\begin{cases} \gamma_{\mathrm{SY17}} = 0.228 \times \left(\dfrac{H_0}{L_{0,\mathrm{SY}}}\right)^{0.108} \cdot \left\{1 - \exp\left[-1.5\pi\dfrac{d}{L_{0,\mathrm{SY}}}\left(1 + 15m^{4/3}\right)\right]\right\} \Big/ \dfrac{d}{L_{0,\mathrm{SY}}} \\ L_{0,\mathrm{SY}} = 0.865L_0 \end{cases} \tag{16}$$

Table 5
Summary of the scatter index and the relative bias by using the G10 formula and Eq. (10). Cases are divided into three groups according to the beach slopes. The better result of each case is shown in bold. The average value of the relative bias is after taking the absolute value.

Group	Name	Source	Beach slope	Scatter Index (%)		Relative Bias (%)	
				G10	Eq. (10)	G10	Eq. (10)
I	B02B	Baldock and Huntley (2002)	1:10	**6.3**	6.4	0.4	**0.3**
	B02C		1:10	7.8	**7.4**	−1.1	**−0.6**
	Guza2	Wu et al. (1985)	1:16	12.4	**7.9**	11.0	**−2.9**
	BJ78	Battjes and Janssen (1978)	1:20	**8.5**	8.5	**4.3**	5.3
	Guza6	Wu et al. (1985)	1:21	11.2	**9.9**	7.0	**7.3**
	Eldeberky	Eldeberky (2011)	1:34	7.0	**3.6**	3.4	**0.3**
	BS85	Battjes and Stive (1985)	1:40	14.6	**3.4**	−13.7	**−2.4**
II	Laboratory	This study	1:100	10.9	**3.3**	−10.2	**−0.8**
	Laboratory		1:200	6.7	**3.2**	−5.8	**0.2**
	Laboratory		1:300	6.6	**3.4**	−5.7	**−1.1**
III	Jensen1	Jensen (2004)	Reef flat	14.2	**4.6**	11.0	**1.1**
	Jensen4		Reef flat	13.3	**2.4**	11.8	**2.0**
	Jensen18		Reef flat	19.2	**11.4**	14.1	**3.3**
	Jensen29		Reef flat	11.7	**5.5**	10.8	**3.8**
Average				10.8	**5.8**	7.9	**2.2**
Standard deviation				3.8	**2.8**	8.9	**2.9**

Table 6
Summary of the scatter index and the relative bias by using the five breaker index models. Cases are divided into four groups according to the beach slopes. The best model of each case is shown in bold. The average value of the relative bias is after taking the absolute value.

Group	Name	Sources	Beach slope	Scatter Index (%)					Relative Bias (%)				
				Eq. (10)	LS17	SA15	BJ78	SY17	Eq. (10)	LS17	SA15	BJ78	SY17
I	B02B	Baldock and Huntley (2002)	1:10	**6.4**	6.5	9.2	6.3	7.8	**0.3**	0.5	2.6	−2.2	1.0
	Guza2	Wu et al. (1985)	1:16	7.9	**7.8**	20.4	12.4	10.1	**−2.9**	4.2	14.1	7.3	3.4
	BJ78	Battjes and Janssen (1978)	1:20	8.5	10.7	10.7	**4.9**	9.7	5.3	7.0	6.8	**2.5**	6.3
	Guza6	Wu et al. (1985)	1:21	**9.9**	13.4	12.9	11.8	10.1	**7.3**	12.0	11.5	10.2	7.4
	Eldeberky	Eldeberky (2011)	1:34	**3.0**	6.1	5.8	3.6	6.2	**0.3**	3.0	2.6	−0.3	1.1
	BS85	Battjes and Stive (1985)	1:40	3.4	**2.5**	2.8	2.7	3.0	−2.4	0.8	**−0.8**	−1.0	−2.0
	BIT7	Zhang and Zou (2012)	1:40	**5.6**	8.6	9.6	13.9	9.4	**4.8**	6.3	6.5	9.2	6.7
	R13a	Ruessink et al. (2013)	1:80	**3.5**	4.2	4.7	3.9	4.1	**2.8**	3.2	3.3	3.1	3.0
II	Laboratory	This study	1:100	**3.3**	10.3	10.6	4.7	3.4	**−0.8**	−9.4	−9.8	3.4	1.7
	Laboratory		1:200	**3.2**	16.6	13.1	7.9	3.9	**0.2**	−16.2	−12.6	7.4	2.4
	Laboratory		1:300	**3.4**	17.9	14.7	7.6	4.3	**−1.1**	−17.5	−14.2	7.0	3.1
III	Jensen1	Jensen (2004)	Reef flat	**4.6**	7.4	7.9	23.1	22.3	**1.1**	4.7	5.5	18.9	18.8
	Jensen4		Reef flat	**2.4**	6.9	7.1	21.5	19.6	**2.0**	6.2	6.4	18.9	17.4
	Jensen18		Reef flat	**11.4**	13.5	14.5	26.6	28.4	**3.3**	8.1	10.0	21.9	24.5
	Jensen29		Reef flat	**5.5**	9.1	9.1	23.4	20.2	**3.8**	8.1	8.2	21.7	18.8
IV	DELILAH	Birkemeier et al. (1997), Reniers et al. (2002) and Reniers and Zijlema (2022)	Field About 1:80	**8.7**	11.3	11.7	11.3	9.2	**3.9**	8.1	8.4	7.9	4.2
Total average				**5.7**	9.5	10.3	11.6	10.7	**2.6**	7.2	7.7	8.9	7.6
Standard deviation				**2.8**	4.3	4.3	8.0	7.7	**2.1**	4.9	4.2	7.4	7.7

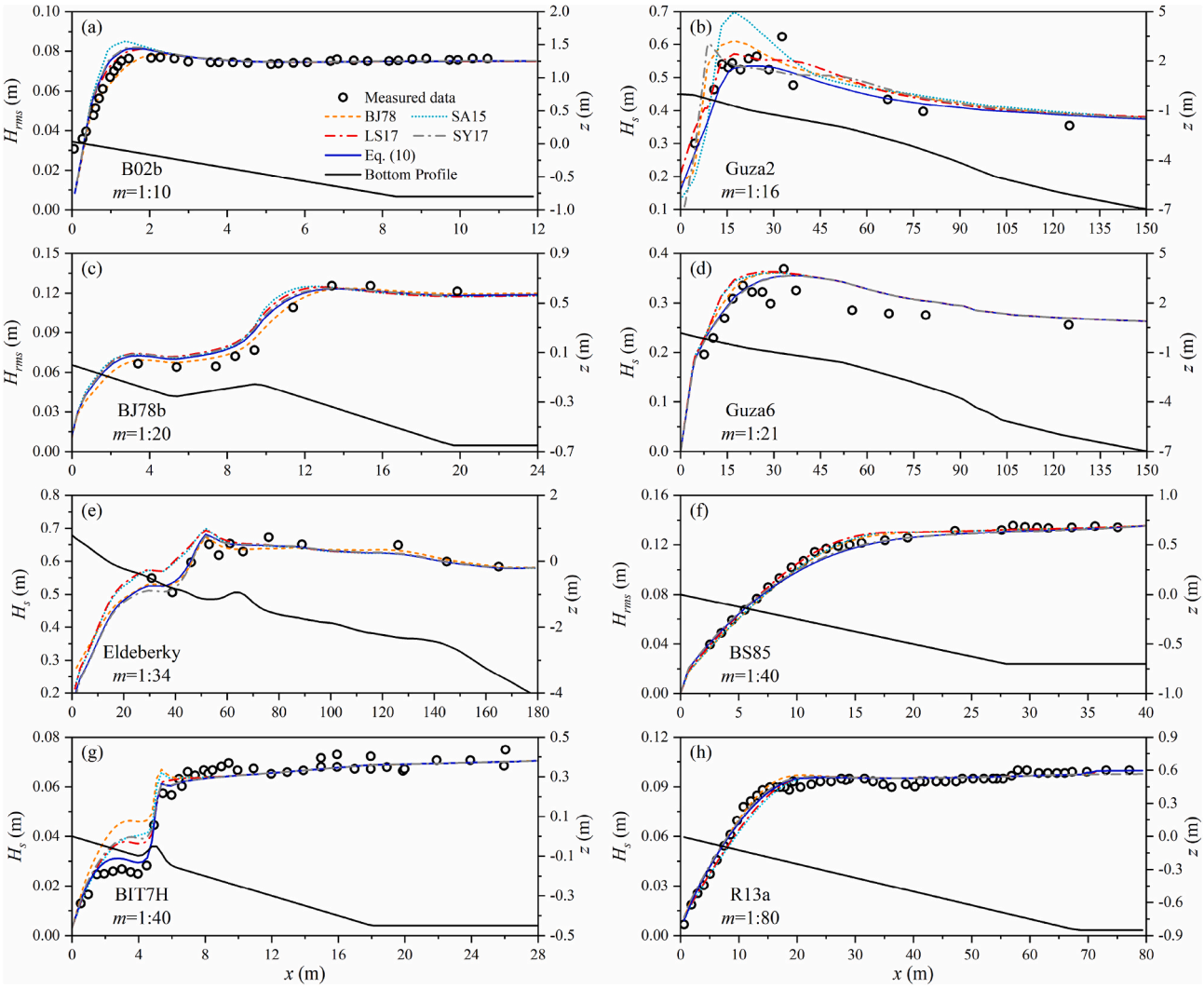

Fig. 8. The simulated wave heights of the five breaker index models under different cases with slopes ranging from 1:10 to 1:80.

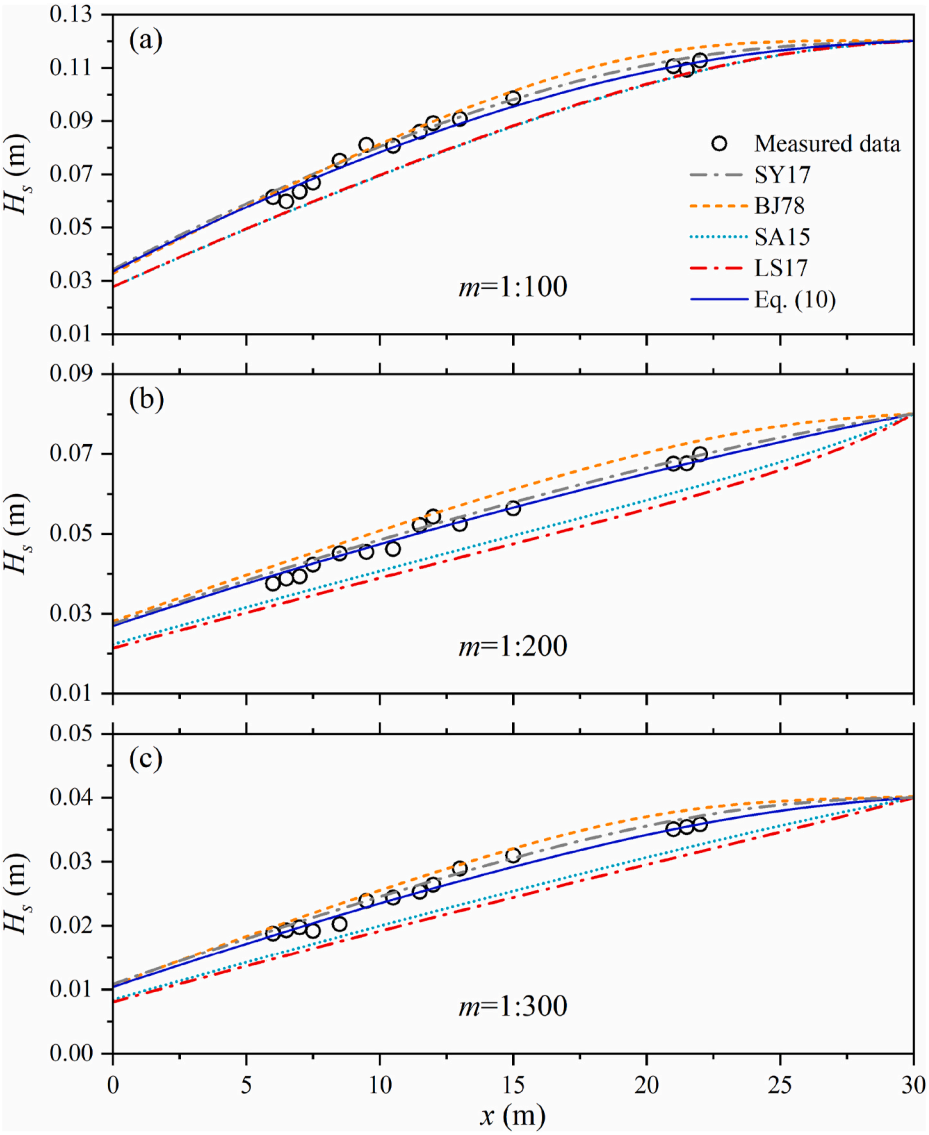

Fig. 9. The simulated wave heights of the five breaker index models under different cases of very mild slopes from 1:100 to 1:300.

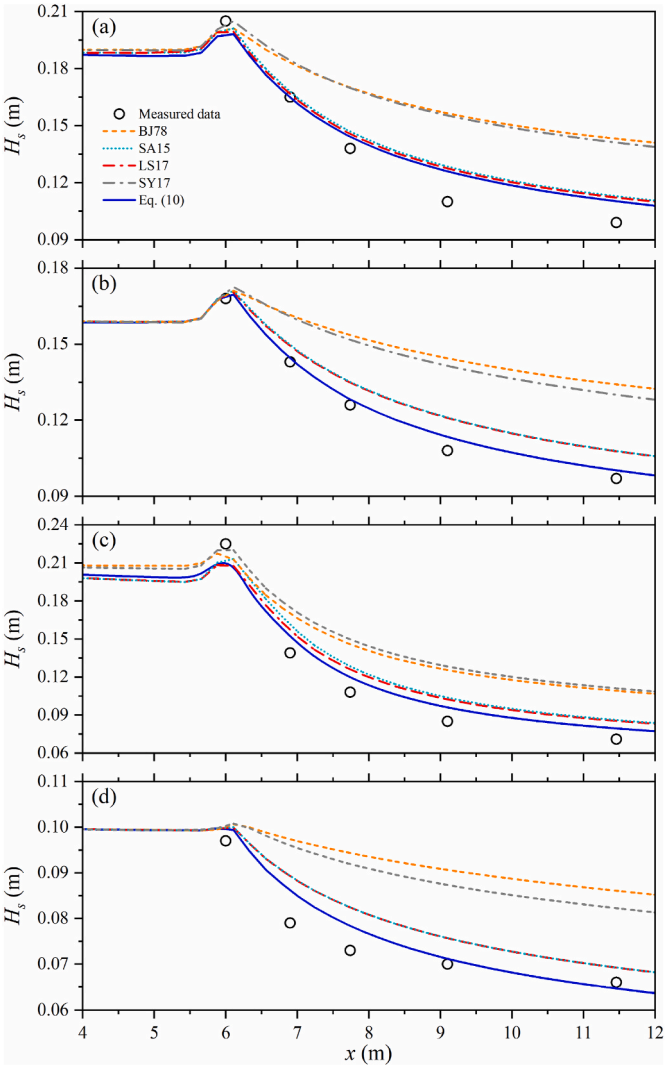

Fig. 10. The simulated wave heights of the five cases in Jensen (2004) by the four models: (a)–(d) are the cases of 1, 4, 18 and 29, respectively. The test bottom profile is shown in Fig. 7.

We choose cases with beach slopes ranging from 1:10 to 1:300 and with deep-water wave steepness varying from 0.0011 to 0.0478. Detailed information on the cases is listed in Table 6.

Following Section 3.2, the comparisons in this section are accomplished based on four groups according to slopes: Group I (m = 1:10–1:80), Group II (m = 1:100–1:300), Group III (m = 0) and Group IV (a field case where m varies with a mean of 1:80). In Group I, the modeled wave heights from all the formulas overall agree well with the observed wave heights (Fig. 8). All the formulas are able to successfully simulate the breaking processes of waves from deep water to shallow water even with variable bathymetry, for example, the cases of Fig. 8(c), (e) and 8(g). The mean scatter index between the modeled and observed wave heights is 7.6% with a standard deviation of 3.9%, and the mean relative bias is 3.9% with a standard deviation of 4.2% (Table 6). At the same time, we also find that the formula from Eq. (10) is better, especially in cases with sandy bars (Fig. 8(e) and (g)), where the scatter index is 4.3% and the relative bias is 2.5%. Comparisons in Group II are shown in Fig. 9. With a slope of 1:100, the modeled wave heights with SA15 and LS17 are slightly lower than those of Eq. (10), while the results of BJ78 and SY17 are slightly higher in deep water and then match those of Eq. (10) in shallow water (Fig. 9(a)). The scatter index of Eq. (10) is 3.3%, and the relative bias is −0.8%. Their magnitudes are lower than the magnitudes of the other four formulas, which have a range of the scatter index from 3.4% to 10.6%, and the relative bias is from −9.8% to 3.4% (Table 6). Similar trends of the comparisons can be found for the slopes of 1:200 and 1:300, while with different scatters and relative biases. In Group III, the wave heights from all the formulas are higher than the observations (Fig. 10). Eq. (10) seems better than others; however, a solid conclusion is difficult to draw due to the limited experimental data. In Group IV, we compared to the model results and observations in a field case which was carried on at Duck, North Carolina (Birkemeier et al., 1997). The variation of the bathymetry and the instrument locations are shown in Fig. 11. We run the five models in with the field cases in the period of 1st −18th October 1990, and the significant wave height along the Delilah array instrument locations (see the locations in Fig. 11) are used for the comparison in the present study in terms of suggestion of Reniers et al. (2002) and Reniers and Zijlema (2022). As we can see, all the formulas can successfully simulate the breaking processes (Fig. 12). Eq. (10) has the scatter index is 8.7% and the relative bias is 3.9%, which are both smaller than those of the remaining four formulas. Overall, the comparisons above indicate that the formula of the breaker index suggested in the present study agrees well with previous studies. The formula works well not only over steep slopes but also over mild slopes and flat bottoms.

5. Conclusions

In the present study, we modified Goda's breaker index formula using laboratory experimental data and a wave model with an aim to improve the wave breaking over mild and flat slopes. In the modified formula, the empirical coefficient A is a function of the deep-water wave steepness. The formula is evaluated against observational data, and the evaluation indicates that the averaged scatter index between the observational significant wave heights from Eq. (10) is 5.8%, nearly half of that from the G10 of 10.8%. The corresponding mean relative bias is 2.2% using Eq. (10), less than 30% of the bias with a G10 of 7.9%. The formula is further evaluated by comparing the formula to previously published formulas. All the formulas are able to successfully simulate the breaking processes of waves from deep water to shallow water. For beach slopes ranging from 1:10 to 1:300 and flat slope cases, especially for cases with mild slopes, Eq. (10) shows better performance. The formula has a mean scatter index of 5.7% and a mean relative bias of 2.6%, while the ranges of the scatter index and relative bias are 9.5% ~11.6% and 7.2%~8.9% of the other formulas, respectively.

CRediT authorship contribution statement

Zereng Chen: Experiments, Data collection, Formal analysis, Numerical simulation, Empirical formula, Validation, Visualization, Paper writing. **Qinghe Zhang:** Conceptualization, Writing – review & editing, Formula discussion, Supervision, Funding acquisition. **Yongsheng Wu:** Paper writing and revise, Formula discussion. **Chao Ji:** Software, Formula discussion.

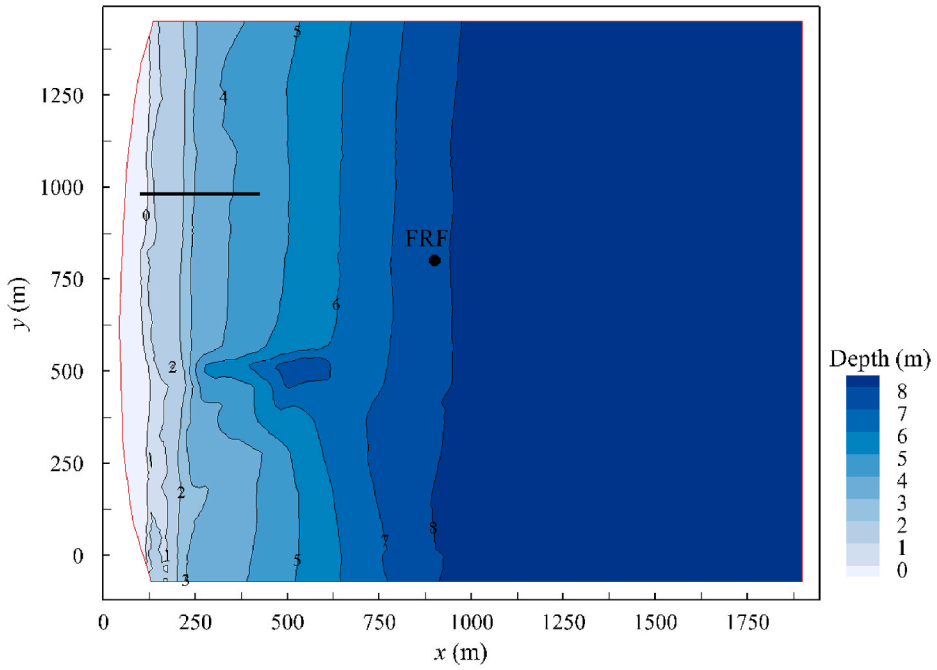

Fig. 11. The bathymetry of Delilah field experiment. Black dot: FRF instrument location. Black line contains the Delilah array instrument locations.

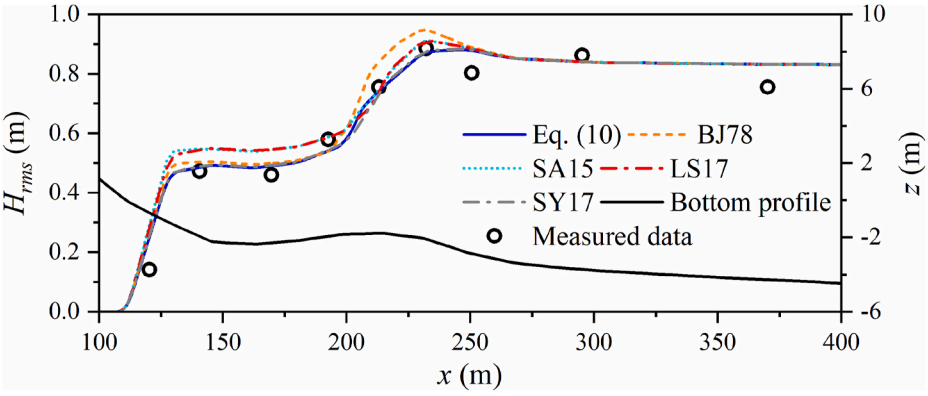

Fig. 12. The simulated wave heights of the five breaker index models alone the Delilah array instrument locations on 10 October for hour 7.

Declaration of competing interest

The authors declare that they have no known competing financial interests or personal relationships that could have appeared to influence the work reported in this paper.

Data availability

No data was used for the research described in the article.

Acknowledgments

This work was supported by the Joint Funds of the National Natural Science Foundation of China (Grant no. U1906231) and the Natural Science Foundation of Tianjin (Grant No.19JCZDJC40200).

References

Allsop, N., Durand, N., Hurdle, D., 1998. Influence of steep seabed slopes on breaking waves for structure design. Coastal Engineering 906–919. https://doi.org/10.1061/9780784404119.067.

Alsina, J.M., Baldock, T.E., 2007. Improved representation of breaking wave energy dissipation in parametric wave transformation models. Coastal Engineering 54 (10), 765–769. https://doi.org/10.1016/j.coastaleng.2007.05.005.

Apotsos, A., Raubenheimer, B., Elgar, S., Guza, R.T., 2008. Testing and calibrating parametric wave transformation models on natural beaches. Coastal Engineering 55 (3), 224–235. https://doi.org/10.1016/j.coastaleng.2007.10.002.

Baldock, T.E., Holmes, P., Bunker, S., Weert, P.V., 1998. Cross-shore hydrodynamics within an unsaturated surf zone. Coastal Engineering 34, 173–196. https://doi.org/10.1016/S0378-3839(98)00017-9.

Baldock, T.E., Huntley, D.A., 2002. Long-wave forcing by the breaking of random gravity waves on a beach. Proc. Royal Soc. London. Series A: Math. Phys. Eng. Sci. 458 (2025), 2177–2201. https://doi.org/10.1098/rspa.2002.0962.

Battjes, J.A., Janssen, J.P.F.M., 1978. Energy Loss and Set-Up Due to Breaking of Random Waves. Proceedings of the 16th International Conference on Coastal Engineering, ASCE, pp. 569–587. https://doi.org/10.1061/9780872621909.034.

Battjes, J.A., Stive, M.J.F., 1985. Calibration and verification of a dissipation model for random breaking waves. J. Geophys. Res. 90 (C5), 9159–9167. https://doi.org/10.1029/JC090iC05p09159.

Birkemeier, W.A., Donoghue, C., Long, C.E., Hathaway, K.H., Baron, C.F., 1997. 1990 DELILAH Nearshore Experiment: Summary Report. Technical report CHL-97-4-24, Field Res. Facil., U. S. Army Eng. Waterw. Exp. Stn., Vicksburg, Miss.

Booij, N., Ris, R.C., Holthuijsen, L.H., 1999. A third-generation wave model for coastal regions 1. Model description and validation. J. Geophys. Res. 104 (C4), 7649–7666. https://doi.org/10.1029/98JC02622.

Camenen, B., Larson, M., 2007. Predictive formulas for breaker depth index and breaker type. J. Coast Res. 23 (4), 1028–1041. https://doi.org/10.2112/05-0566.1.

Choi, J., Lee, J.-I., Yoon, S.B., 2012. Surface roller modeling for mean longshore current over a barred beach in a random wave environment. J. Coast Res. 284, 1100–1120. https://doi.org/10.2112/JCOASTRES-D-10-00151.1.

Choi, J., Yoon, S.B., 2011. Numerical simulation of nearshore circulation on field topography under random wave environment. Coastal Engineering 58 (5), 395–408. https://doi.org/10.1016/j.coastaleng.2010.12.002.

Deborah J Wood, M.M., Oumeraci, Hocine, 2001. The SWAN model used to study wave evolution in a flume. Ocean Eng. 28 (7), 805–823. https://doi.org/10.1016/S0029-8018(00)00033-0.

Eldeberky, Y., 2011. Modeling spectra of breaking waves propagating over a beach. Ain Shams Eng. J. 2 (2), 71–77. https://doi.org/10.1016/j.asej.2011.07.002.

Goda, Y., 1975. Irregular wave deformation in the surf zone. Coast. Eng. Japan 18 (1), 13–26. https://doi.org/10.1080/05785634.1975.11924196.

Goda, Y., 2009. A performance test of nearshore wave height prediction with clash datasets. Coastal Engineering 56 (3), 220–229. https://doi.org/10.1016/j.coastaleng.2008.07.003.

Goda, Y., 2010. Reanalysis of regular and random breaking wave statistics. Coast Eng. J. 52 (1), 71–106. https://doi.org/10.1142/S0578563410002129.

Holthuijsen, L.H., 2007. Waves in Oceanic and Coastal Waters. Cambridge University Press, New York, NY, USA.

Izumiya, T., Isobe, M., 1986. Breaking criterion on non-uniformly sloping beach. Coastal Engineering 1 (20), 318–327. https://doi.org/10.9753/icce.v20.25.

Jensen, M.S., 2004. Breaking of Waves over a Steep Bottom Slope. Aalborg: Hydraulics & Coastal Engineering Laboratory, 2 ed. Department of Civil Engineering, Aalborg University (Series Paper; No. 22).

Kang, H., Chun, I., Oh, B., 2020. New procedure for determining equivalent deep-water wave height and design wave heights under irregular wave conditions. Int. J. Nav. Archit. Ocean Eng. 12, 168–177. https://doi.org/10.1016/j.ijnaoe.2019.09.002.

Kriebel, D., 2000. Breaking Waves in Intermediate-Depths with and without Current. Coastal Engineering 2000 (Proc. Int. Conf., Sydney), ASCE, pp. 203–215. https://doi.org/10.1061/40549(276)16.

Li, Y., Tu, Y., Cui, L., Dong, G., 2000. Transformation and breaking of irregular waves on very gentle slope. China Ocean Eng. 14 (3), 261–278. https://doi.org/10.3321/j.issn:0890-5487.2000.03.001.

Lin, P., Liu, P.L.-F., 1998. A numerical study of breaking waves in the surf zone. J. Fluid Mech. 359, 239–264. https://doi.org/10.1017/S002211209700846X.

Lin, S., Sheng, J., 2017. Assessing the performance of wave breaking parameterizations in shallow waters in spectral wave models. Ocean Model. 120, 41–59. https://doi.org/10.1016/j.ocemod.2017.10.009.

Lin, S., Sheng, J., Ohashi, K., Song, Q., 2021. Wave-current interactions during hurricanes earl and igor in the northwest atlantic. J. Geophys. Res.: Oceans. https://doi.org/10.1029/2021JC017609, 2021JC017609.

Lin, S., Sheng, J., Xing, J., 2020. Performance evaluation of parameterizations for wind input and wave dissipation in the spectral wave model for the northwest Atlantic ocean. Atmos.-Ocean 58 (4), 258–286. https://doi.org/10.1080/07055900.2020.1790336.

Liu, Y., Niu, X., Yu, X., 2011. A new predictive formula for inception of regular wave breaking. Coastal Engineering 58 (9), 877–889. https://doi.org/10.1016/j.coastaleng.2011.05.004.

Mase, H., Kirby, J.T., 1992. Hybrid frequency-domain KdV equation for random wave transformation. Coastal Engineering 474–487. https://doi.org/10.1061/9780872629332.035.

Mendez, F.J., Losada, I.J., 2004. An empirical model to estimate the propagation of random breaking and nonbreaking waves over vegetation fields. Coastal Engineering 51 (2), 103–118. https://doi.org/10.1016/j.coastaleng.2003.11.003.

Nelson, R.C., 1987. Design wave heights on very mild slopes–an experimental study. Transactions of the Institution of Engineers, Australia. Civ. Eng. 29 (3), 157–161.

Rattanapitikon, W., Duong, N., 2019. Parametric wave models for computing statistical-based and spectral-based root-mean-square wave heights. Int. Conf. Asian Pacific Coasts 681–686. https://doi.org/10.1007/978-981-15-0291-0_93.

Reniers, A.J.H.M., Van Dongeren, A.R., Battjes, J.A., Thornton, E.B., 2002. Linear modeling of infragravity waves during Delilah. J. Geophys. Res.: Oceans 107 (C10), 1–18. https://doi.org/10.1029/2001jc001083, 10.

Reniers, A.J.H.M., Zijlema, M., 2022. SWAN SurfBeat-1D. Coastal Engineering 172 (3), 104068. https://doi.org/10.1016/j.coastaleng.2021.104068.

Robertson, B., Gharabaghi, B., Hall, K., 2015. Prediction of incipient breaking wave-heights using artificial neural networks and empirical relationships. Coast Eng. J. 31 (2), 150901234203000 https://doi.org/10.1142/S0578563415500187.

Ruessink, B.G., Michallet, H., Bonneton, P., Mouazé, D., Lara, J., Silva, P.A., Wellens, P., 2013. Globex: wave dynamics on a gently sloping laboraty beach, 2013 Proc. Coast. Dynam. 1351–1362. https://dspace.library.uu.nl/handle/1874/310236.

Ruessink, B.G., Walstra, D.J.R., Southgate, H.N., 2003. Calibration and verification of a parametric wave model on barred beaches. Coastal Engineering 48 (3), 139–149. https://doi.org/10.1016/S0378-3839(03)00023-1.

Sakai, S., Hirayama, K.-i., Saeki, H., 1988. A new parameter for wave breaking with opposing current on sloping sea bed. Coastal Engineering 1 (21), 1035–1044. https://doi.org/10.9753/icce.v21.77.

Salmon, J.E., Holthuijsen, L.H., 2015. Modeling depth-induced wave breaking over complex coastal bathymetries. Coastal Engineering 105 (11), 21–35. https://doi.org/10.1016/j.coastaleng.2015.08.002.

Salmon, J.E., Holthuijsen, L.H., Zijlema, M., van Vledder, G.P., Pietrzak, J.D., 2015. Scaling depth-induced wave-breaking in two-dimensional spectral wave models. Ocean Model. 87, 30–47. https://doi.org/10.1016/j.ocemod.2014.12.011.

Salvadori, G., Tomasicchio, G.R., D'Alessandro, F., 2014. Practical guidelines for multivariate analysis and design in coastal and off-shore engineering. Coastal Engineering 88 (6), 1–14. https://doi.org/10.1016/j.coastaleng.2014.01.011.

Shen, Y., Zhang, Q., Chen, C., Ji, C., 2017. Application of modified breaking index of Goda in SWAN model. Port. Eng. Technol 54 (6), 1–6. https://doi.org/10.16403/j.cnki. ggjs20170601 (in Chinese).

Svendsen, I.A., 1984. Wave heights and set-up in a surf zone. Coastal Engineering 8 (4), 303–329. https://doi.org/10.1016/0378-3839(84)90028-0.

Ting, F.C., 2001. Laboratory study of wave and turbulence velocities in a broad-banded irregular wave surf zone. Coastal Engineering 43 (3–4), 183–208. https://doi.org/10.1016/S0378-3839(01)00013-8.

Tomasicchio, G.R., Mahmoudi Kurdistani, S., D'Alessandro, F., Hassanabadi, L., 2020. Simple wave breaking depth index formula for regular waves. J. Waterw. Port, Coast. Ocean Eng. 146 (1), 06019001 https://doi.org/10.1061/(ASCE)WW.1943-5460.0000539.

Udo, K., Mano, A., 2010. Backshore coarsening processes triggered by wave-induced sand transport: the critical role of storm events. Earth Surf. Process. Landforms 35 (11), 1269–1280. https://doi.org/10.1002/esp.1951.

Varing, A., Filipot, J.F., Grilli, S., Rui, D., Yates, M., 2020. A new definition of the kinematic breaking onset criterion validated with solitary and quasi-regular waves in shallow water. Coastal Engineering 164 (1), 103755. https://doi.org/10.1016/j.coastaleng.2020.103755.

Wu, C., Thornton, E.B., Guza, R.T., 1985. Waves and longshore currents: comparison of a numerical model with field data. J. Geophys. Res. 90 (C3), 4951–4958. https://doi.org/10.1029/JC090iC03p04951.

Yao, Y., Huang, Z., Monismith, S.G., Lo, E.Y.M., 2013. Characteristics of monochromatic waves breaking over fringing reefs. J. Coast Res. 29 (1), 94–104. https://doi.org/10.2112/JCOASTRES-D-12-00021.1.

Zhang, C., Li, Y., Cai, Y., Shi, J., Zheng, J., Cai, F., Qi, H., 2021. Parameterization of nearshore wave breaker index. Coastal Engineering 168, 10394. https://doi.org/10.1016/j.coastaleng.2021.103914.

Zhang, Z., Zou, Z., 2012. Vertical distribution of longshore currents over plane and barred beaches. J. Hydrodyn. 24 (5), 718–728. https://doi.org/10.1016/S1001-6058(11)60296-5.